Astron. Astrophys. 339, 545–552 (1998)

ASTRONOMY AND ASTROPHYSICS

α Centauri: coronal temperature structure and abundances from ASCA observations

R. Mewe[1], S.A. Drake[2], J.S. Kaastra[1], C.J. Schrijver[3], J.J. Drake[4], M. Güdel[5], J.H.M.M. Schmitt[6], K.P. Singh[7], and N.E. White[2]

[1] Space Research Organization Netherlands (SRON), Sorbonnelaan 2, 3584 CA Utrecht, The Netherlands
[2] Code 660, Laboratory for High Energy Astrophysics, NASA/GSFC, Greenbelt, MD 20771, USA
[3] Stanford-Lockheed Inst. for Space Research, Department H1-12, Bldg. 252, 3251 Hanover St., Palo Alto, CA 94304-1191, USA
[4] Smithsonian Astrophysical Observatory, 60 Garden St., Cambridge, MA 02138, USA
[5] Paul Scherrer Institut, Würenlingen und Villigen, CH-5232 Villigen PSI, Switzerland
[6] Max-Planck-Institut für Extraterrestrische Physik, Postfach 1603, D-85740 Garching, Germany
[7] Tata Institute of Fundamental Research, Homi Bhabha Road, Mumbai 400 005, India

Received 16 July 1997 / Accepted 31 August 1998

Abstract. We have analyzed the X-ray spectrum of the nearby binary α Cen AB (G2V + K1V) that has been obtained from observations with ASCA. The coronal temperature structure and abundances have been derived from multi-temperature fitting and confirmed by a differential emission measure analysis. The corona as seen by ASCA is essentially isothermal with a temperature around 0.3 keV, consistent with the evolutionary picture of coronae of aging solar-type stars. A comparison between the measurements from various instruments indicates a source variability in the coronal flux (which precludes the joint fitting of data from different instruments taken at different epochs) and temperature structure consistent with that discovered in a series of ROSAT observations. The elemental abundances agree with solar photospheric abundances for Ne, Si, and Fe at 1σ level, while O appears to be underabundant by a factor of about 3 relative to solar photospheric values, and Mg overabundant by a factor of a few. The abundance ratios with respect to Fe are better determined: [O/Fe] = 0.4$\pm$0.14 ($\times$ solar, etc.), [Mg/Fe] = 4$\pm$1, [Ne/Fe] = 1$\pm$0.3, and [Si/Fe] = 6$\pm$4.

Key words: stars: coronae – stars: individual: α Cen – stars: abundances – X-rays: stars

1. Introduction

The Sun is a moderately old (4.6 Gyr) G2 V star, with an X-ray luminosity L_X typically in the range $\sim 5\ 10^{26}$ to $\sim 2\ 10^{27}$ erg/s in the EINSTEIN IPC band (Schmitt et al. 1990, Schmitt 1997) that is close to the median value for single G dwarf stars found in the survey of Maggio et al. (1987). Extreme-ultraviolet (EUV) and soft X-ray studies of the Sun have shown that the bulk of the quiet solar corona is at a temperature of $\sim$ 0.1-0.3 keV, while the plasma above active regions is found to be at $\sim$ 0.3-0.6 keV (e.g., Withbroe 1988, Brosius et al. 1996). During flares hotter plasma with a temperature of $\sim$ 0.6-3 keV is detected (e.g., Feldman et al. 1996). An interesting feature of the solar corona is that its plasma is often characterized by non-photospheric abundances. For α Cen this has been studied by Drake et al. (1997).

The EUVE and ASCA observations of stars much more active than the Sun (e.g., Drake 1996a, White 1996) have provided the following results: (i) active stars have coronae with fundamentally different temperature structures than the solar corona, in that they have significant persistent components at temperatures $T \sim$ 1-4 keV; (ii) the line-to-continuum contrast (mainly from Fe) seen in both the EUV and soft X-ray spectra of such stars is weaker than predicted by thermal plasma models assuming solar photospheric abundances by factors of $\sim$ 2-10, at least for RS CVn stars and Algols (e.g., Drake et al. 1994, Schrijver et al. 1995, Singh et al. 1995, 1996) and the pre-main-sequence star AB Dor (Mewe et al. 1996). Various explanations for the observed relatively weak line-to-continuum ratio have been suggested (cf. Sect. 6.2.). As noted by Drake (1996b) and Singh et al. (1996), all of these explanations except for a low metal abundance are inadequate to explain the line-to-continuum problem found in the soft X-ray spectral region of most, but not all, active stars for which high-quality spectra have been obtained.

With ROSAT, EUVE, and ASCA Güdel et al. (1997a,b) have studied spectra of a series of solar-type stars (i.e. single G dwarfs) of different ages and established that (i) relatively old (like the Sun) solar-type dwarfs have coronae dominated by plasma at $\sim$ 0.3 keV similar to the active Sun, and (ii) the more active (and younger) G dwarfs (like EK Dra) have coronae with both $\sim$ 0.3 keV and $\gtrsim$ 1 keV plasmas.

The closest G or K dwarfs to the Sun are, in fact, the two stars in the wide visual binary α Cen that lie at a distance of 1.34 pc. In this paper we discuss the ASCA spectrum of α Cen, derive a coronal model that fits the observed spectrum, and then compare the results of this analysis with the results based on measurements with ROSAT, EUVE, and SAX.

Send offprint requests to: R. Mewe, (R.Mewe@sron.nl)

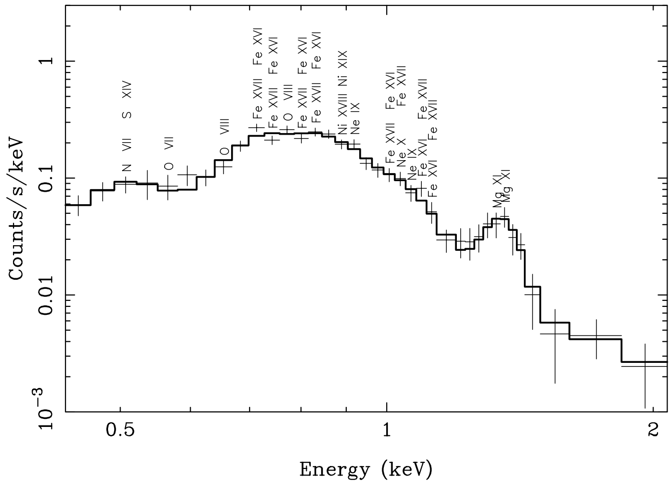

Fig. 1. Observed and fitted (thick solid line) ASCA SIS0 spectrum of α Cen, corrected for background, for a 1-T fit with non-solar abundances (Table 1). Error bars indicate $\pm 1\sigma$ errors of the observations. Prominent lines containing more than 20 counts as predicted by the best-fit model are indicated by the ions from which they originate.

2. The target star

The binary α Cen AB lies at a distance of 1.34 pc and consists of a $1.1 M_\odot$ G2 V star with radius $1.24 R_\odot$ and a $0.9 M_\odot$ K1 V star with radius $0.84 R_\odot$ (e.g., Flannery and Ayres 1978). These stars appear to be a little (10%) older (age 5-6 Gyr) and of somewhat higher metallicity ($Z \sim 1.3 - 2.0 Z_\odot$) than the Sun (e.g., Lydon et al. 1993, Furenlid and Meylan 1990, Smith et al. 1986, Chmielewski et al. 1992). The orbit is so wide (semi-major axis 23.5 AU = 17.5 $''$, period 80.1 yr, see Flannery and Ayres 1978) that no significant tidal or magnetic interaction between the two components is expected.

A systematic search for stellar coronae in X-rays was done for the first time with the Astronomical Netherlands satellite (ANS) which provided the discovery of X-rays from Sirius and a corona around Capella, but yielded for α Cen only a 3σ upper limit of $\log L_X < 27.2$ in the 0.2-0.284 keV band (Mewe et al. 1975). The latter source was first detected by Nugent and Garmire (1978) with the A-2 experiment on HEAO-1 with an X-ray luminosity $\log L_X$ = 27.5 in the 0.1-0.5 keV band. For other X-ray observations we refer to Sect. 6.1.

3. Observations

The source α Cen was observed by the Advanced Satellite for Cosmology and Astrophysics ASCA (see Tanaka et al. 1994 for a brief description) on 1996 February 27 from 02:42 UT to 20:40 UT. Data were obtained with both pairs of Solid State Imaging Spectrometers (hereafter SIS) and Gas Imaging Spectrometers (GIS), but for the purposes of the present analysis we have used only the SIS spectra because the source spectrum is very soft and declines steeply, being below the background level at energies above ~ 2.5 keV. A net SIS exposure time of 25.0 ks was obtained with a total counting rate of 0.113 c/s. We have made fits to both SIS0 and SIS1 data and get the same results within the uncertainties; the results discussed in Sect. 5 are those obtained using the SIS0 data.

The SIS detectors are described in detail in Burke et al. (1991) and their properties have been summarized, e.g., in Singh et al. (1996). One update to these descriptions is a result of the degradation of the spectral resolution of the SIS CCD's due to radiation damage: this has been discussed recently by Dotani et al. (1996). At the time of the α Cen observation by ASCA, we estimate that the SIS spectral resolution had degraded from 6% to 10% FWHM at 1 keV. The response matrix that we generated as part of the analysis of this spectrum took account of this effect. The SIS data were selected as described in Singh et al. (1996) using the NASA software package FTOOLS/XSELECT. To accumulate the source spectrum, we have extracted all events in a circle of about 6.5$'$ diameter centered on the α Cen source, while we have accumulated the background spectrum from a source-free region of the CCD.

For the spectral analysis, we have ignored the 14 data points below 0.433 keV and 432 datapoints above 2.075 keV (which contain too much background and comprise less than 1.3% of all counts). Then all energy bins above about 1.4 keV were rebinned into 4 bins to ensure a sufficient signal-to-noise ratio S/N per bin, i.e. N $\gtrsim$ 15-20 cts/bin which yields a spectrum of 37 bins between 0.433-2.075 keV. To account for systematic uncertainties in the calibration of the effective detector area (cf. Fig. 5 of Dotani et al. 1996) we have added systematic uncertainties to the bins around the O K edge feature (1-9 between 0.433-0.698): 10,25,20,15,10,7,5% for bins 1-3,4,5,6,7,8,9, respectively. To the last two bins above the Si K edge at 1.74 keV (36,37 between 1.608-2.075 keV) we added 5% uncertainties. Finally, because a small offset does seem to be present in the SIS spectrum, we have applied a gain offset of -20 eV.

4. Spectral fitting

For our primary spectral analysis, we have used the SPEX software package (Kaastra et al. 1996a). This package contains models for the calculation of spectra from optically thin plasmas in collisional ionization equilibrium (CIE) (Mewe et al. 1985, 1986; Kaastra and Mewe 1993). Recently the calculations for the Fe-L complexes have been updated using results from the HULLAC code (Liedahl et al. 1995) and various other improvements have been made (cf. Mewe et al. 1995b). We express abundances relative to the solar photospheric values taken from Anders and Grevesse (1989). For the ionization balance we use Arnaud and Rothenflug (1985) for all elements except iron, for which we use the update of Arnaud and Raymond (1992). Emission measures are defined here as $EM = \int n_\mathrm{e} n_\mathrm{H} \mathrm{d}V$, where n_e is the electron density, n_H is the hydrogen density and V the emitting plasma volume. Galactic absorption is taken into account using the model of Morrison and McCammon (1983). As a check of the results obtained using SPEX, we have repeated some of the spectral analysis using the independent spectral analysis package XSPEC. We obtained essentially the same results using XSPEC, so we will not further discuss the XSPEC spectral analysis.

4.1. DEM modeling

We assume that the spectra emitted by stellar coronae can be approximated by linear combinations of spectra of isothermal plasmas: if stellar coronae are optically thin, then all components are observed as emitted, regardless of where they occur on the disk or, in the case of binaries, on which binary component they occur. We introduce the differential emission measure $D(T) = n_{\rm e}(T) n_{\rm H}(T) dV/d\log T$. This is the weighting function that describes the contribution by the plasma, at each temperature, to the observed spectrum. In our models we implicitly assume thermal ionization equilibrium, thus ignoring possible transient effects, and we ignore effects that depend on the plasma density, which affects only a few lines, i.e. we consider the low-density limit. To derive physical parameters from the spectra various techniques can be applied such as multi-temperature fitting or fitting with continuous models to derive $D(T)$ (for a detailed description of various DEM analysis techniques implemented in SPEX, e.g. Gauss fitting method or Chebyshev polynomial technique, we refer to Kaastra et al. 1996b and Mewe et al. 1996). The DEM distribution is derived by matching the observed spectrum as well as possible to a synthesized model spectrum for a given temperature grid. We display the results as the emission measure integrated over a temperature bin, i.e. $DEM = D(T)\Delta\log T$ so that the total emission measure within a certain temperature range follows by summing the values of DEM for the relevant temperature bins.

Table 1. Abundance ratios for the corona of α Cen relative to the corresponding solar photospheric abundance ratios of Anders and Grevesse (1989)[1] as derived from ASCA & EUVE observations and compared with corresponding values adopted for the average solar corona

	Abundance ratio		
	ASCA[2]	EUVE[3]	Solar Corona[4]
[O/Fe]	0.38±0.14		0.34
[Ne/Fe]	1.0±0.3	0.32±0.08	0.36
[Mg/Fe]	4.4±1.0		1.4
[Al/Fe]		1.9±0.9	1.4
[Si/Fe]	5.8±4.2	1.8±1.0	1.3
[S/Fe]		1.1±0.2	0.43
[Ca/Ne]		2.7±5.4	3.8

[1] Abundance values in logarithmic units, with $\log_{10}$H=12.00: O, 8.93; Ne, 8.09; Mg, 7.58; Al, 6.47; Si, 7.55; S, 7.21; Ca, 6.36; Fe, 7.67; these values are a little (0.2 dex, for Fe 0.04 dex) smaller than the abundances adopted by Drake et al. (1997) for the photospheres of α Cen AB.

[2] This work.

[3] Drake et al. (1997) based on line ratios given in their Table 6; the DEM in their Fig. 7 indicates [S/Fe] to be lower by a factor of $\sim$ 3.

[4] Feldman et al. (1992).

5. Results

Because the fits are not sensitively dependent on the interstellar hydrogen column density we used a fixed value of $N_{\rm H} = 10^{18}$ cm^{-2} which is approximately equal to the best-fit value Mewe et al. (1995a) obtained in the analysis of the EUVE spectrum of α Cen.

5.1. Temperature and abundance analysis

We first attempted to fit the spectrum with one- and two-temperature models using solar photospheric abundances but obtained very poor fits with minimum χ^2 of 72 and 50 (35 and 33 d.o.f.), respectively. Using non-solar abundances for the most important elements improves the fit considerably. In this case it turns out that a single-temperature model is sufficient because adding of more temperature components does not improve the fit significantly.

Elements for which relatively strong, isolated lines are present in the spectrum yield the most reliable abundances. In the ASCA spectrum of α Cen the abundance of O is most accurately determined from the 0.65 keV Lyman α line which is a relatively strong line with an intensity of 163 counts according to the best-fit model. The Fe abundance is determined by the Fe L-shell $\sim$ 1 keV complex, mainly the Fe XVII lines at 0.73, 0.82, and 1.02 keV with a total intensity of 713 counts. The abundance of Ne is derived from the He-like Ne IX line at 0.92 keV (230 counts), which however is just in the middle of the Fe L feature so that the Ne abundance is strongly correlated to the Fe abundance. The He-like Mg XI line at 1.34 keV (83 counts) constrains the Mg abundance, while the Si abundance is rather weakly constrained by the He-like Si XIII line at 1.85 keV (7 counts). The contribution from the continuum in the spectral bins where these lines are formed is always only a few percent ($\sim$ 3-5%). No dominant lines with sufficient S/N ratios were present to constrain the other elemental abundances. The N abundance cannot be constrained due to calibration problems around 0.5 keV (Dotani et al. 1996). For these elements the abundances were fixed to solar photospheric values. The resulting best-fit values are for the temperature T = 0.27 $\pm$ 0.03 keV and for the emission measure EM = (5.3 $\pm$ 1.0) 10^{49} cm^{-3}, with minimum χ^2 = 20.0 (30 d.o.f.). The observed ASCA SIS0 spectrum, corrected for the background together with the best-fit 1-T model is shown in Fig. 1.

The best-fit abundances with respect to the corresponding solar photospheric values of Anders and Grevesse (1989) are: O: 0.30±0.11; Ne: $0.79^{+0.58}_{-0.37}$; Mg: $3.4^{+2.6}_{-1.5}$; Si: $4.5^{+6.9}_{-3.5}$; Fe: $0.77^{+0.37}_{-0.23}$. The abundances agree with solar photospheric abundances for Ne, Si, and Fe at 1σ level, while O is underabundant by a factor of about 3 relative to solar photospheric values, and Mg is overabundant by a factor of 3.4. For solar-type stars Mg has come out to be overabundant in several observations (Güdel et al. 1997a,b).

The abundances relative to hydrogen are poorly constrained because in this soft spectrum with only little high-energy flux the pure continuum in the spectrum is too weak to form a good reference. But the abundance ratios relative to Fe are much more robust. We have checked this by fixing the Fe abundance to its best-fit value of 0.77 and varying the other abundances and determining the uncertainties in the ratios to the Fe abundance. The abundance ratios relative to Fe with respect to the corresponding solar abundance ratios are given in Table 1. We remark that the given uncertainties are lower limits because the effects of systematic errors in the atomic data (excitation rates and ionization balance) can probably not always be neglected and in the case of the Ne abundance the effect of blending with the Fe L-shell complex.

5.2. DEM analysis

In reconstructing the DEM we have applied a multi-temperature Gauss fitting method with a number of Gaussian temperature components of finite width (characterized by the "standard deviation" σ, where $2.35{\times}\sigma$ is the FWHM on a $\log T$ scale). We use a temperature grid between 0.01-10 keV with $\Delta \log T$=0.1 and adopt the set of abundances given in Table 1. By varying the abundances step by step it turns out that this set of abundances is also the optimal one for the DEM analysis. For an acceptable fit one component is sufficient and we obtain χ^2 = 20.0 (34 d.o.f.) for a narrow (σ = 0.014) Gaussian component at 0.27 keV and total emission measure of 5.4 10^{49} cm^{-3} (cf. Fig. 2), consistent with the result of Sect. 5.1. The analysis of the ASCA spectrum does not require any significant DEM component above about 0.4 keV up to 10 keV. This result is confirmed by a fit with 8 Chebyshev polynomials (χ^2 = 20.4, 29 d.o.f.) (cf. Fig. 2). The DEM shown in Fig. 2 has a peak temperature comparable to that of the coronal emission measure distribution of the solar-like star χ^1 Ori as determined by

Schrijver et al. (1995) from EUVE observations. It is comparable to the emission measure distribution of a modestly active region on the Sun (e.g., Raymond and Doyle 1981, Dere 1982, Bruner and McWhirter 1988, Doschek and Cowan 1984, Dere and Mason 1993). Notice that the emission in the ASCA energy band of the average solar corona if viewed as a star (i.e. without no angular resolution) would be dominated by such active regions during the majority of the solar cycle.

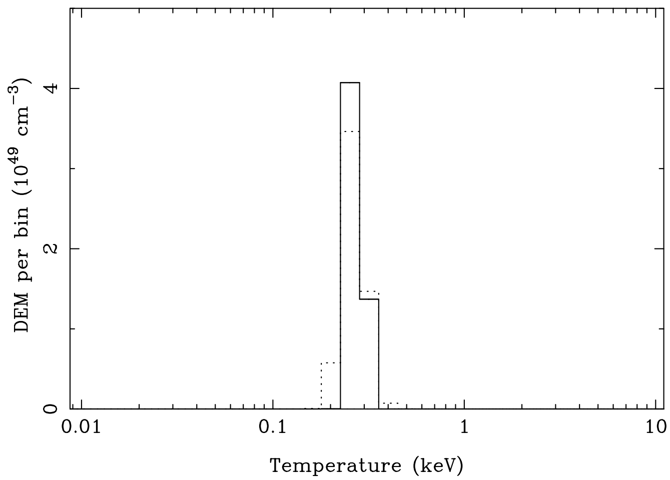

Fig. 2. The DEM (the emission measure per temperature bin) for the ASCA SIS0 spectrum using the Multi-Gauss method with one temperature component and with non-solar abundances (Table 1) (solid line). For comparison the result of a polynomial fit is presented as a dotted line.

6. Discussion

6.1. Source variability; temperature structure and X-ray luminosity

Schmitt (1998) has reported the results of a monitoring campaign on α Cen carried out by ROSAT on a daily basis over about one month. The HRI resolved the X-ray emission of the two components A and B of α Cen (angular separation $\sim 18''$), and each component displayed an overall variability of about a factor of two: the light curve of the G2 V star (comp. A) exhibited a wavelike modulation, while that of the K1 V star (B) displayed a more erratic behaviour, with evidence of occasional flaring. The X-ray flux of B was on average about twice that of A.

A comparison by Schmitt (private communication) of three ROSAT PSPC spectra taken at different times between 1992 and 1994 reveals that the three spectra cannot be fit by one single spectral model, but instead exhibit a variation of a factor of 2-3 in the soft (0.1-0.4 keV) region and a much larger variability (3-$\gtrsim$ 30) in the hard (0.5-2 keV) band that overlaps with the ASCA spectral range. From the position of the centroid of the PSPC image Schmitt attributed the high hard-band signal to a flare on the component B which interpretation is supported by the frequent detection of flare-like variability in the HRI light curve of α Cen B.

Such a type of variability is consistent with the known flux and spectral variability of the Sun during its activity cycle (e.g., up to a factor $\sim$ 100 in the SOLRAD 9 spectral band of 0.6-1.5 keV, cf. Pallavicini 1993). It is thus expected that weakly active solar-type stars such as α Cen will show large variations in X-ray luminosity on a long-term (yearly) basis, due to activity changes over their magnetic cycles. In addition, since only a modest portion of the surface of such stars will be covered with active regions, the evolution of individual active regions and, in particular, their rotational modulation, as they rotate onto and out of the visible hemisphere, may dramatically change the X-ray flux on a timescale of ≤ 1 day to weeks. The observed X-ray variability of α Cen is also consistent with the detected chromospheric and transition-region UV line emission variability (of up to $\sim$ 30%) of both α Cen A and B (e.g., Ayres et al. 1995, Char et al. 1993), which has been attributed to rotational modulation (with periods of about 23 and 37 days for components

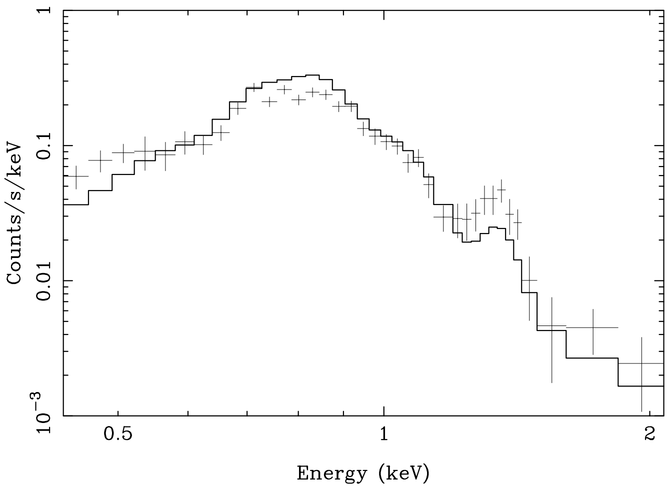

Fig. 3. Predicted ASCA SIS spectrum of α Cen (thick solid line) for the EUVE coronal model of Drake et al. (1997), but multiplied by a factor of 0.3, compared to the ASCA observations (crosses).

A and B, respectively, cf. Jay et al. 1997, Guinan and Messina 1995).

Can the ASCA obervations be compared with other soft X-ray and EUV observations? A difficulty in comparing observations from different instruments is, apart from intercalibration problems and incomplete models (e.g., missing lines in the EUV in the modelling codes), the fact that different instruments have different energy passbands, and that, for coronal sources, this restricts the plasma temperatures to which they are sensitive. For example, the ROSAT data and part of the EUVE spectrum are dominated by a soft ($T \approx 0.1$ keV) plasma component (see below) to which ASCA is essentially blind.

Our result obtained from the ASCA data can therefore be considered only as an idealization of the true continuous coronal temperature structure. On the Sun, broad emission measures are dominated by contributions from bright, non-isothermal loops in the lower corona. Such structures have a typical density of $\sim 10^9$ cm^{-3} comparable to that derived by Drake et al. (1997) and Mewe et al. (1995a) from the EUVE spectrum for the corona of α Cen and could therefore be expected for α Cen as well. Therefore, the narrowness of our DEM reconstruction in our view merely indicates that our data with a limited S/N ratio and limited spectral resolution can be satisfactorily represented by such a structure. It does not necessarily imply that higher-resolution devices would find other temperature intervals outside our DEM to be devoid of emission measure. We believe, however, that our DEM solution indicates the amount and average temperature of the most dominating portions of a structured corona emitting at energies visible by ASCA ($\gtrsim$ 0.4 keV, i.e. hot active regions).

If the source is not intrinsically variable, or when simultaneous measurements by different instruments are available, then a unique description of the coronal emission should exist in principle, even though any single instrument would not be able to find that entire solution, being insensitive to other parts of the spectral and thus temperature domain. For example, Mewe et al. (1996) were able to jointly fit the simultaneous EUVE and ASCA spectra of AB Dor. However, such a procedure is not possible for the non-simultaneous EUVE and ASCA observations of α Cen, simply because of the strong source variability (factor of $\gtrsim$ 3). Fig. 3 illustrates this. We compare the observed ASCA SIS spectrum to the model spectrum predicted by the DEM derived by Drake et al. (1997) from the EUVE observations for their coronal model (their Fig. 8, lower panel, abundances corresponding to last column of our Table 1), using the ionization balance of Arnaud and Rothenflug (1985) also for Fe. The model spectrum has been renormalized by multiplication by a factor of 0.3. (We note that the remaining differences in the spectra can be probably explained above about 1 keV by differences in the temperature structure and/or in the abundances, and around 0.5 keV by calibration effects). Because of this strong source variability we abandoned a further detailed comparison between the EUVE and ASCA results (e.g., emission measure models).

Though a joint fitting and detailed modelling of data from different instruments taken at different epochs is precluded for a variable X-ray source such as α Cen, a crude comparison between the various derived X-ray fluxes and temperature structures for α Cen gives results that are generally consistent with the type of variability seen by ROSAT alone. We compare the X-ray luminosity L_X[1] as derived from different instruments (in parentheses observation date; instrument passband in keV; L_X): EINSTEIN (26 Aug. 1979; 0.15-4; 4) (Golub et al. 1982), ROSAT (2-3 Sep. 1992; 0.1-2.4; 3) (Schmitt 1997), EUVE (29 May- 1 June 1993; 0.016-0.18; 6) (Mewe et al. 1995a, Drake et al. 1997), ASCA (27 Feb. 1996; 0.4-10; 1), and SAX (23-24 Feb. 1997; 0.1-10; 3) (Mewe et al. 1998). This comparison indicates that the X-ray luminosity of α Cen varies by at least a factor of several on a timescale of ≤ 1 year.

We now briefly discuss the coronal temperature structure of α Cen as inferred from the various EUV and soft X-ray observations. The EUVE spectrum can be approximately described by a 2-T model ($T = 0.10 \pm 0.01$ keV and 0.22 ± 0.04 keV with EM's in the ratio about 1 : 3) where the high temperature is close to that ($T = 0.27 \pm 0.03$ keV) derived from the ASCA observations, while the low-temperature component is consistent with the ROSAT HRI observation (with a hardness ratio of -0.88 corresponding to $T \sim$ 0.1-0.13 keV, cf. Fig. 2 of Berghöfer et al. 1996). ASCA is essentially blind for such a soft component because most of the flux emitted by such a component is concentrated in the 0.1-0.4 keV band. The EINSTEIN IPC observations also implied a rather soft ($T = 0.18 \pm 0.34$ keV) spectrum (cf. Golub et al. 1982) at this early epoch of observation. Finally, the results of recent SAX LECS observations (Mewe et al. 1998) yield a soft ($T = 0.09 \pm 0.01$ keV) component similar to the soft EUVE and ROSAT components, and a $T = 0.5 \pm 0.1$ keV component somewhat higher in temperature than the hotter EUVE component, but which for SAX has an emission measure that is about six times weaker than that

[1] (in 10^{27} erg/s normalized to the ROSAT PSPC (0.1-2.4 keV) energy band which overlaps at least part of all other energy bands)

of the soft component. Although comparison of temperatures inferred from instruments with different bandpasses and spectral resolutions is even more fraught with possible systematic efforts than the comparison of fluxes, these various measurements are suggestive of variations of the coronal temperature structure, particularly the higher temperature part of the DEM, similar to those seen in the individual ROSAT PSPC spectral measurements (Schmitt, priv. comm.).

From a study in X-rays of the age evolution of solar-type stars Güdel et al. (1997b) have established a general decay in activity as well as a softening of the spectrum with increasing age or decreasing rotation period. We expect for α Cen with an age of 5-6 Gyr a dominant coronal temperature in the range $\sim$ 0.17-0.32 keV (within the 1σ error bars), at least for the A-component (G-star). Although in our observations we cannot separate the G-star from the twice brighter K-star we can at least give from our resulting DEM an upper limit consistent with that expected for a solar-like star about as old as the Sun. To make definite conclusions about the coronal properties of the solar-type G-component we have to wait for spatially resolved spectral observations of the two α Cen components with the low-energy transmission grating (LETG) on AXAF.

6.2. Abundances

Meyer (1985) and Feldman (1992) have reviewed the subject of non-photospheric solar coronal abundances and present evidence that the solar corona, wind, and energetic particles all exhibit a similar pattern of abundances, namely an underabundance of elements with high first-ionization potential (FIP) values ($E_{ion} \gtrsim 8$ eV) relative to elements with lower FIP values by factors of $\sim$ 1-10, depending on the types of coronal structure observed. The quiet corona, including evolved active regions, and slow solar wind show a steady low FIP enhancement of about a factor of 4. The "FIP Effect" in the full-disk solar spectrum has received less attention, partly because of a lack of full-disk observations. This is unfortunate because it is only full-disk observations that can be compared directly to stellar observations. However, Laming et al. (1995) have recently re-analyzed 25 year-old EUV spectra of the solar corona and find evidence for a factor of 3-4 enhancement in low-FIP elements (compared to their photospheric values). This enhancement was only observed in $T \geq 0.1$ keV plasma. As discussed by Laming et al. (1995), the enhancement of low FIP elements at these temperatures is consistent with what one would expect when the full-disk emission is dominated by active regions. At lower temperatures, the dominant emission is that observed to concentrate at supergranular boundaries. Laming et al. (1995) concluded that this supergranulation emission does not exhibit a significant enhancement of low FIP elements.

A commonly suggested explanation (e.g., Feldman and Widing 1990, McKenzie and Feldman 1992, von Steiger and Geiss 1989) for these anomalous abundances is that they are due to a preferential siphoning of ions as compared to neutrals into the corona from out of the lower chromosphere ($T \leq 10^4$K) by some process that is not yet well understood. Other processes are also possible such as suggested by Sheely (1996) in which neutrals are driven out of magnetic loops as they form and evolve from the chromosphere. Though solar spectra generally do not seem to show evidence for gravitational settling it is interesting to note that van den Oord and Mewe (1998) show that in principle effects on the abundances can occur due to the density stratification caused by gravitational setting in coronal loops.

Drake et al. (1997) have analyzed the same EUVE spectrum of α Cen as Mewe et al. (1995a) did and found a similar emission measure distribution below 1 keV.[2] They have investigated the coronal composition and concluded by comparing derived emission measures and measured line ratios of elements with low and high FIP that the coronal regions which dominate the EUV spectrum appear to be characterized by a solar-like FIP effect (for the first time for a solar-like star other than the Sun with similar activity): low-FIP elements (Mg, Al, Si, Ca, and Fe) are overabundant relative to the high-FIP elements (O, Ne, and S) by a factor $\sim$ 2-3. From their quoted abundance ratios we derive the corresponding ratios relative to solar photospheric ratios presented in Table 1.

If we compare these EUVE results with those inferred from the analysis of the ASCA spectrum (Table 1) we see that the abundance ratios are different.[3] In both sets we see indications of a FIP effect but the detailed correspondence for a given element is rather poor. If we compare our results with those for the average solar corona (Table 1) we notice that the O/Fe ratio is consistent with a FIP effect (which was also found by Drake et al. (1997), see their Fig. 7), that Mg is clearly overabundant (Güdel et al. 1997a,b found with ASCA for three single solar-type stars Mg to be twice overabundant, while the other abundances were solar), while Si and Ne may be solar photospheric although the Ne result may be affected by blending in the Fe L-shell complex. If we compare the abundance ratios with respect to another element (e.g., Ne) to those in parentheses for the Sun we obtain: [O/Ne]=0.4$\pm$0.2 (0.9), [Mg/Ne]=4.4$\pm$1.7 (3.9), [Si/Ne]=5.8$\pm$4.5 (3.6). These ratios are in agreement except for O/Ne. One may infer that the abundances of either O or Ne are different from their solar photospheric values. If O deviates, then the close similarity between the solar and α Cen's O/Fe ratio suggests that both O and Fe are 'underabundant' by the same factor ($\sim$ 2.5) relative to the solar corona, contradicting, however, what we expect from a FIP effect. But we should note that ASCA is sensitive to active regions in which the abundances 'anomalies' are expected to be most variable.

What effects could influence the determination of the abundances from different instruments? Mewe et al. (1995a) and

[2] Drake et al. found the maximum DEM at a slightly lower temperature (0.19 keV) than Mewe et al. (0.23 keV), while the difference in scale (factor $\sim$ 6) is easily explained by the fact that Drake et al. took $\Delta \log T = 0.3$ instead of 0.1, and corrected the DEM by a factor of 2 accounting for the fact that only half of the coronal photons are seen which, however, is only true for a low-height, homogeneous corona.

[3] Using the Arnaud-Rothenflug ionization balance also for Fe as Drake et al. (1997) did in their analysis of the EUVE spectrum we obtain from the ASCA spectrum the same results (within the error bars) as those given in Table 1.

Drake et al. (1997) found from the EUVE spectrum similar DEM distributions below about 1 keV; the first authors found a problem at higher temperatures. In order to fit the whole spectrum including the EUVE SW continuum the Mewe et al. models had to invoke a high-temperature ($\gtrsim 2$ keV) component in order to match the line-continuum ratio. Drake et al. (1997) did not encounter this problem because they derived their relative abundances solely from line ratios and therefore did not constrain the continuum intensity level.

The presence of such a hot component can be ruled out by the observations with the other instruments, but Mewe et al. (1995a) and Schrijver et al. (1995) suggested that several effects could be responsible for the relatively weak line-to-continuum ratio observed in the EUVE spectrum such as the depletion of metal abundances (important for ASCA spectra of the more active RS CVn stars, but probably less important for the weaker stars), the omission of many weak lines in the current plasma codes which together may form a "pseudo-continuum" just in the EUVE SW band (Schmitt et al. 1996, Drake et al. 1997), or optical-depth effects (Schrijver et al. 1994, 1995). For α Cen probably only a few strong lines in the EUV region are marginally optically thick (Mewe et al. 1995a). Because optical depths scale with wavelength we expect that in the ASCA band scattering effects are less important. Lacking further information, we neglect these effects in the determination of the ASCA abundances although we know from spectral observations of solar active regions that such effects can play a role (e.g., for the Fe XVII 15.015 Å line [Phillips et al. 1997]), and probably even in disk-averaged spectra because of the asymmetric distribution of active regions over the stellar disk.

The hypothesis that there are missing lines in the EUV (70-140 Å) wavelength band is being investigated by Liedahl et al. (1998) who are performing calculations with the Livermore HULLAC code in this band where lines of the Fe M-shell and Ne to S L-shell complexes are formed. As an early result, they have obtained for the ion Fe IX a significantly larger (~ 3 times) flux in this wavelength region than that predicted in the current version of the SPEX code (Liedahl et al. 1998).

Though all these effects can influence the derived abundances there is at the moment no unique explanation for the different abundances derived from different observations and the possibility remains that they are due to systematic errors that are affecting one or both of the abundance determinations. However, we note that for the Sun (and by analogy probably also for α Cen) elemental abundances can differ between young active-region loops and older quiet loops (e.g., Feldman 1992). As a result this may affect, even when averaging over the entire disk, the mean coronal abundance as the balance between quiet and active regions shifts through the solar cycle. We must conclude that the ASCA abundances derived in this study show some indications for a possible FIP effect (as previously inferred from the EUVE analysis), but that in order to better constrain the absolute abundances relative to hydrogen and the relative [Ne/Fe] abundance (both of which are presently inconsistent with their FIP effect values) a high S/N ratio and spectral resolution, broad-band pass AXAF observation is highly desirable. In fact, it would be even more desirable if multiple AXAF observations at widely separated intervals (years, say) were obtained, so that the present evidence for variability of the coronal abundances (based on observations by different instruments at epochs separated by a few years) could be either confirmed or refuted.

Acknowledgements. Part of this work was made possible by the support of the Space Research Organization of the Netherlands (SRON). JJD was supported by the AXAF Science Center NASA contract NAS8-39073 during the course of this research. We thank Dr. Martin Laming for helpful comments.

References

Anders E., Grevesse N., 1989, Geochimica et Cosmochimica Acta 53, 197
Arnaud M., Raymond J., 1992, ApJ 398, 394
Arnaud M., Rothenflug R., 1985, A&AS 60, 425
Ayres T.R., Fleming, T.A., Simon, T. et al., 1995, ApJS 96, 223
Berghöfer T.W., Schmitt J.H.H.M., Cassinelli J.P., 1996, A&AS 118, 481
Brosius J.W., Davila J.M., Thomas R.J., Monsignori-Fossi B.C., 1996, ApJS 106, 143
Bruner M.E., McWhirter R.W.P., 1988, ApJ 326, 1002
Burke B.E., Mountain R.W., Harrison D.C. et al., 1991, IEEE Trans., ED-38, 1069
Char S., Foing B.H., Beckman J. et al., 1993, A&A 276, 78
Chmielewski Y., Friel E., Cayrel de Strobel G., Bentolila C., 1992, A&A 263, 219
Dere K.P., 1982, Solar Phys. 77, 77
Dere K.P., Mason H.E., 1993, Solar Phys. 144, 217
Doschek G.A., Cowan R.D., 1984, ApJS 56, 67
Dotani T., Mitsuda K., Ezuka H. et al., 1996, ASCA Newsletter No. 4, p. 3
Drake J.J., 1996a, in: Pallavicini R., Dupree A.K. (eds.), Cool Stars, Stellar Systems, and the Sun, PASP Conf. Series, p. 203
Drake J.J., Laming J.M., Widing K.G., 1997, ApJ 478, 403
Drake S.A., 1996b, in: Holt S.S., Sonneborn G. (eds.), Cosmic Abundances, ASP, San Francisco, p. 215
Drake S.A., Singh K.P., White N.E., Simon T., 1994, ApJ 436, L87
Feldman U., 1992, Phys. Scr. 46, 202
Feldman U., Doschek G.A., Behring W.E., Phillips K.J.H., 1996, ApJ 460, 1034
Feldman U., Widing K.G., 1990, ApJ 363, 292
Feldman U., Mandelbaum P., Seely J.F., Doschek G.A., Gursky H., 1992, ApJS 81, 387
Flannery B.P., Ayres T.R., 1978, ApJ 221, 175
Furenlid I, Meylan T., 1990, ApJ 350, 827
Golub L., Harnden Jr. F.R., Pallavicini R. et al., 1982, ApJ, 253, 242
Güdel M., Guinan E.F., Mewe R. et al., 1997a, ApJ, 479, 416
Güdel M., Guinan E.F., Skinner S.L., 1997b, ApJ, 483, 947
Guinan E., Messina S., 1995, IAU Circular 6259
Jay J.E., Guinan, E.F., Morgan, N.D. et al., 1997, BAAS 29, 730
Kaastra J.S., Mewe R., 1993, Legacy, 3, 16
Kaastra J.S., Mewe R., Liedahl D.A. et al., 1996b, A&A 314, 547
Kaastra J.S., Mewe R., Nieuwenhuijzen, H., 1996a, in: Yamashita K., Watanabe T. (eds.), UV and X-ray Spectroscopy of Astrophysical and Laboratory Plasmas, Universal Academy Press, Inc., Tokyo, p. 411
Laming J.M., Drake J.J., Widing K.G., 1995, ApJ 443, 416

Liedahl D.A., Mewe, R., Kaastra J.S., 1998, in preparation
Liedahl D.A., Osterheld A.L., Goldstein W.H., 1995, ApJ 438, L115
Lydon T.S., Fox P.A., Sofia S., 1993, ApJ 413, 390
Maggio A., Sciortini S., Vaiana G.S. et al., 1987, ApJ, 315, 687
Mewe R., Gronenschild E.H.B.M., van den Oord G.H.J., 1985, A&AS 62, 197
Mewe R., Güdel M., Favata F., Kaastra J.S., 1998, A&A, in press
Mewe R., Heise, J., Gronenschild E.H.B.M. et al., 1975, ApJ, 202, L67
Mewe R., Kaastra J.S., Liedahl D.A., 1995b, Legacy 6, 16
Mewe R., Kaastra J.S., Schrijver C.J. et al., 1995a, A&A 296, 477
Mewe R., Kaastra J.S., White S.M., Pallavicini R., 1996, A&A 315, 170
Mewe R. Lemen J.R., van den Oord G.H.J., 1986, A&AS 65, 511
Meyer J.-P., 1985, ApJS 57, 151& 172
Morrison R., McCammon D., 1983, ApJ 270, 119
Nugent J., Garmire G., 1978, ApJ 226, L83
Pallavicini R., 1993, in: Linsky J.F., Serio S. (eds.), Physics of Solar and Stellar Coronae, Kluwer Acad. Publ., Dordrecht-Holland, p. 237
Phillips K.J.H., Greer, C.J., Bhatia A.K., Keenan, F.P., 1997, ApJ 469, L57
Raymond J.C., Doyle J.G., 1981, ApJ 245, 1141
Schmitt J.H.M.M., 1997, A&A 318, 215
Schmitt J.H.M.M., 1998, in: Donahue R., Bookbinder J.A. (eds.), Cool Stars, Stellar Systems, and the Sun, Astron. Soc. of the Pacific, San Francisco, in press
Schmitt J.H.M.M., Collura A., Sciortini et al., 1990, ApJ 365, 704
Schmitt J.H.M.M., Drake J.J., Stern R.A., 1996, ApJ 465, L51
Schrijver C.J., van den Oord G.H.J., Mewe R., 1994, A&A 289, L23
Schrijver C.J., van den Oord G.H.J., Mewe R., Kaastra J.S., 1995, A&A 302, 438
Sheely N.R., 1996, ApJ 469, 423
Singh K.P., Drake S.A., White N.E., 1995, ApJ 445, 840
Singh K.P., White N.E., Drake S.A., 1996, ApJ 456, 766
Smith G., Edvardsson B., Frisk U., 1986, A&A 165, 126
Tanaka Y., Inoue H., Holt S.S., 1994, PASJ, 46, L37
van den Oord G.H.J., Mewe R., 1998, in preparation for A&A
von Steiger R., Geiss J., 1989, A&A 225, 222
White N.E., 1996, in: Pallavicini R., Dupree A.K. (eds.), Cool Stars, Stellar Systems, and the Sun, PASP Conf. Series, p. 193
Withbroe G.L., 1988, ApJ, 325, 442